PHYSICAL REVIEW B **68**, 012506 (2003)

# Evidence for the coupling between $\gamma$-band carriers and the incommensurate spin fluctuations in $Sr_2RuO_4$

Ping Lou,[1,2] Ming-Che Chang,[1] and Wen-Chin Wu[1]
[1]*Department of Physics, National Taiwan Normal University, Taipei 11650, Taiwan*
[2]*Department of Physics, Anhui University, Hefei 230039, Anhui, People's Republic of China*
(Received 14 January 2003; published 25 July 2003)

The normal-state transport properties are investigated for $Sr_2RuO_4$ both in and out of the $RuO_2$ plane. It is shown that a quantitatively consistent explanation of $\rho_{ab}$ and $\rho_c$ can be obtained by assuming that, in addition to the normal scattering of electrons by impurities and the electron-electron scattering, there is a strong coupling between the carriers of $\gamma$ band and the incommensurate spin fluctuations peaked at $\mathbf{Q}_i=(\pm0.6,\pm0.6)\pi/a$. In order to test this model, we suggest a pressure-dependent resistivity measurement to be performed.

DOI: 10.1103/PhysRevB.68.012506 PACS number(s): 74.25.Gz, 74.20.Mn, 72.15.−v, 71.27.+a

It is known that the only perovskite superconductor without Cu element $Sr_2RuO_4$ shows novel behaviors for the normal-state in-plane ($\rho_{ab}$) and out-of-plane ($\rho_c$) resistivities. $\rho_{ab}$ exhibits a Fermi-liquid behavior up to $T_{\rm FL}\simeq 25$ K and above this temperature shows a monotonous rise with a curvature weaker than $T^2$; while $\rho_c$ is metallic at $T<T_M \simeq 130$ K, and becomes nonmetallic at $T>T_M$.[1,2] Several mechanisms have been suggested for the novel behaviors. For $\rho_{ab}$, much emphasis has been placed on the ferromagnetic spin fluctuations, which has been used to interpret $\rho_{ab}$ data in support of the possible microscopic origin of the quantum phase transition,[3] or the $p$-wave superconductivity in $Sr_2RuO_4$.[4] While for $\rho_c$, emphasis has been placed on the thermally assisted hopping, in support of the picture that two-dimensional ferromagnetic spin fluctuations are enhanced by pressure.[5]

Here we explore an alternative mechanism, in which the $\rho_{ab}$ anomaly originates from the scattering by incommensurate spin fluctuations (ISF's), meanwhile, the interlayer hopping assisted by the same ISF leads to the $\rho_c$ anomaly. It should be noted that recent inelastic neutron scattering (INS) studies of the spin dynamics in $Sr_2RuO_4$ have unambiguously revealed the presence of strong ISF peaked at $\mathbf{Q}_i=(\pm0.6,\pm0.6)\pi/a$ in $RuO_2$ planes.[6,7] Although previous theoretical works[3–5] focused on the mechanism of the carrier scattering by *ferromagnetic* spin fluctuations, up to now, however, INS measurement does not see any sizeable ferromagnetic spin fluctuations for $RuO_2$.[6,7] Furthermore, as suggested in a recent work,[8] even if there is a ferromagnetic spin fluctuation, it should be weaker than the incommensurate spin fluctuation. Therefore, we expect naturally that there is a strong coupling between the carriers of $Sr_2RuO_4$ and the incommensurate spin fluctuations. We shall show that it is due to this coupling that leads to the anomalous resistivity behavior of $Sr_2RuO_4$ both in plane and out of plane.

We first investigate the resistivity anomaly in the $ab$ plane. There are three ($\alpha$, $\beta$, $\gamma$) bands in $Sr_2RuO_4$. Assuming interband transition is weak, hence $\rho^i_{ab}(T)=\rho^i_n(T)+\rho^i_{\rm SF}(T)$ for a given band $i$. Here $\rho^i_n(T)\equiv a+bT^2$ represents the Fermi liquid behavior together with the impurity scattering,[9] while $\rho^i_{\rm SF}(T)$ is the resistivity arising due to the coupling between the carriers of $RuO_2$ planes and the incommensurate spin fluctuations (instead of the ferromagnetic spin fluctuations). As usual, the formula used to calculate $\rho_{\rm SF}(T)$ is derived from the force-force correlation in memory-function approximation[10–12]

$$\rho_{\rm SF}(T)\propto\frac{J^2}{T}\sum_{\mathbf{k}\cdot\mathbf{q}}\left(\frac{\partial\varepsilon_{\mathbf{q+k}}}{\partial q_x}-\frac{\partial\varepsilon_{\mathbf{k}}}{\partial k_x}\right)^2\chi''(\mathbf{q},\varepsilon_{\mathbf{q+k}}-\varepsilon_{\mathbf{k}})[f(\varepsilon_{\mathbf{k}})-f(\varepsilon_{\mathbf{q+k}})]n_B(\varepsilon_{\mathbf{q+k}}-\varepsilon_{\mathbf{k}})[n_B(\varepsilon_{\mathbf{q+k}}-\varepsilon_{\mathbf{k}})+1], \tag{1}$$

where $J$ is the interaction constant that the carriers scattered by the spin fluctuations, $T$ is the temperature, $f(\omega)$ is the Fermi function, and $n_B(\omega)$ is the Bose function. $\partial\varepsilon_{\mathbf{q}}/\partial q_x$ divided by $\hbar$ corresponds to the band velocity along $x$ direction and $\chi''(\mathbf{q},\omega)$ is the spin-fluctuation spectral function, which will be introduced phenomenologically in the following. For two dimensional (2D) system, the sum over $\mathbf{q}$ (or $\mathbf{k}$) in Eq. (1) is replaced by the integral on $\mathbf{q}$ (or $\mathbf{k}$) being taken over the first Brillouin zone.

Here, we introduce the spin-fluctuation spectral function $\chi''(\mathbf{q},\omega)$ used in Eq. (1). For simplicity, we follow Refs. 6,7 to take the phenomenological form

$$\chi''(\mathbf{q},\omega)=\frac{\chi'(\mathbf{Q}_i,0)}{1+\xi^2(\mathbf{q}-\mathbf{Q}_i)^2}\,\frac{\omega\Gamma}{\omega^2+\Gamma^2}, \tag{2}$$

where $\xi$ is the magnetic correlation length, $\Gamma$ is the damping energy, and $\chi'(\mathbf{Q}_i,0)$ is the static spin susceptibility at wave vector $\mathbf{Q}_i$. Here $\mathbf{Q}_i=(\pm0.6,\pm0.6)\pi/a$, corresponding to those incommensurate peaks observed by INS. In the calculation, the parameters $\xi$, $\Gamma$, and $\chi'(\mathbf{Q}_i,0)$ are determined by fitting to the INS experiments (see Fig. 4 of Ref. 6, for example), *without* any adjustment. Thus the only free parameter in Eq. (1) is the interaction constant $J$.

For the energy dispersions, we adopt the following forms for $\alpha$, $\beta$, and $\gamma$ bands:

$$\varepsilon_{\alpha,\beta}(\mathbf{k})=\varepsilon^+_{\mathbf{k}}\mp\sqrt{(\varepsilon^-_{\mathbf{k}})^2+t^2_\perp},\quad \varepsilon_\gamma(\mathbf{k})=\varepsilon^{xy}_{\mathbf{k}}, \tag{3}$$

 

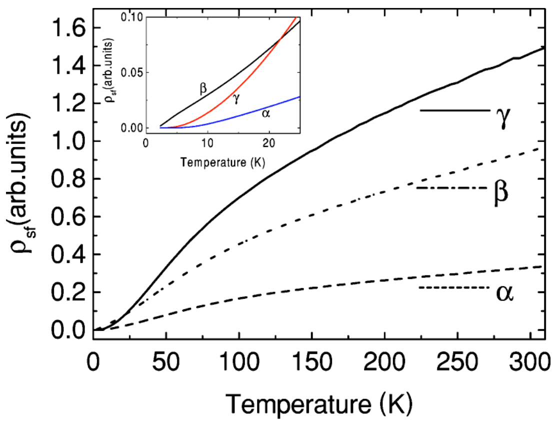


FIG. 1. The in-plane resistivity $\rho_{\mathrm{SF}}(T)$ due to the scattering by incommensurate spin fluctuations vs temperature $T$ for the $\alpha$, $\beta$, and $\gamma$ bands, respectively. Inset shows the low-temperature behaviors more clearly.

where $\varepsilon_{\mathbf{k}}^{\pm} \equiv (\varepsilon_{\mathbf{k}}^{xz} \pm \varepsilon_{\mathbf{k}}^{yz})/2$ and

$$\varepsilon_{\mathbf{k}}^{i} = -2t_x \cos k_x a - 2t_y \cos k_y a + 4t' \cos k_x a \cos k_y a - \mu, \tag{4}$$

with

$$(t_x, t_y, t', \mu) = (0.44, 0.44, -0.14, 0.50),$$
$$(0.31, 0.045, 0.01, 0.24),$$
$$(0.045, 0.31, -0.01, 0.24)\ \mathrm{eV}$$

for $i = xy, xz, yz$ orbital, respectively. The same parameters being fitted to de Haas–van Alphen (dHvA) experiments are also used in Ref. 13. Here $t_\perp = 0.1$ eV is the hybridization between the *xz* and *yz* orbitals which results in hybridized $\alpha$ and $\beta$ bands. For each orbital, $t_x$ ($t_y$) and $t'$ are the nearest and next-nearest neighbor hopping amplitudes and $\mu$ is the chemical potential. In order to examine possible effects that the carriers of the $\alpha$, $\beta$ and $\gamma$ bands interact with the incommensurate spin fluctuations, we calculate $\rho_{\mathrm{SF}}(T)$ for each bands separately and present the results in Fig. 1. It should be emphasized that for easy comparison, here we apply the *same* magnitude of $J$ for all three bands.

From a global perspective, the effect of ISF on $\gamma$ band is stronger than those of $\alpha$ and $\beta$ bands (assuming the same $J$). In the low-temperature regime, the behaviors of temperature-dependent resistivities of $\gamma$ and $\alpha$ bands are quite different from that of $\beta$ band. The resistivities of $\gamma$ and $\alpha$ bands follow *quadratic* temperature dependence, but that of the $\beta$ band displays *linear* temperature dependence, which *cannot* fit the experimental result of $T^2$ law[1,2] (see Fig. 2). In addition, comparing the results of $\alpha$ and $\gamma$ bands, in order to produce the same magnitude of $\rho_{\mathrm{SF}}(T)$, the interaction constant $J$ of the $\alpha$ band needs to be about 2–3 times stronger than that of $\gamma$ band. This seems contradictory with the experimental fact that the mass enhancement of $\alpha$ band is 2–3 times smaller than that of the $\gamma$ band.[14] This gives strong indication that ISF acts most effectively on the carriers of the $\gamma$ band and its effect on $\alpha$ and $\beta$ bands can be safely ignored in $Sr_2RuO_4$.

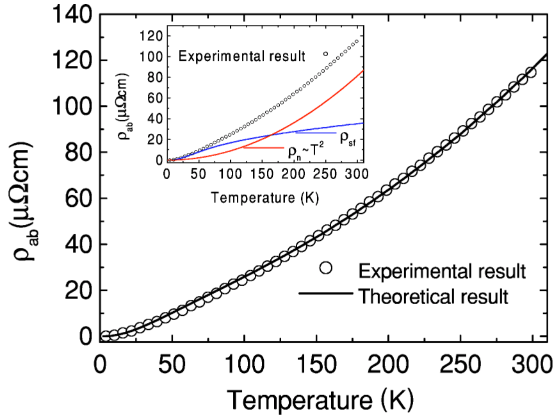


FIG. 2. In-plane resistivity $\rho_{ab}$ vs temperature $T$: open circles are the experimental data (from Ref. 2), while solid lines are the theoretical results. The inset displays the contributions of $\rho_{\mathrm{SF}}$ and $\rho_n = bT^2$ with $b = 9.04 \times 10^{-4}$ $\mu\Omega$ cm/K$^2$ separately, together with the experimental results.

Consequently, we model $\rho_{ab}$ using a weighted sum of $\rho_n = a + bT^2$ and $\rho_{\mathrm{SF}}^{\gamma}$. Here $\rho_n$ includes the contribution from $\alpha$, $\beta$, and $\gamma$ bands altogether (very likely to be dominated by the $\gamma$ band with the largest Fermi surface) due to scattering of the electrons by impurities and by other electrons, while $\rho_{\mathrm{SF}}^{\gamma}$ includes only the contribution of $\gamma$ band. The fit to the experimental data, taken from Ref. 2, is shown in Fig. 2. Almost perfect agreement between experiments and theoretical calculations thus gives us confidence that the ISF is most effectively coupled to the carriers of $\gamma$ band. In the inset of Fig. 2, we display the best fits of $\rho_n(T) = bT^2$ with $b = 9.04 \times 10^{-4}$ $\mu\Omega$ cm/K$^2$ and $\rho_{\mathrm{SF}}^{\gamma}(T)$ separately, together with experimental results. It is evident that the contribution due to impurity scattering is negligibly small in the plane ($a = 0$). We also note that there is a cross point be-

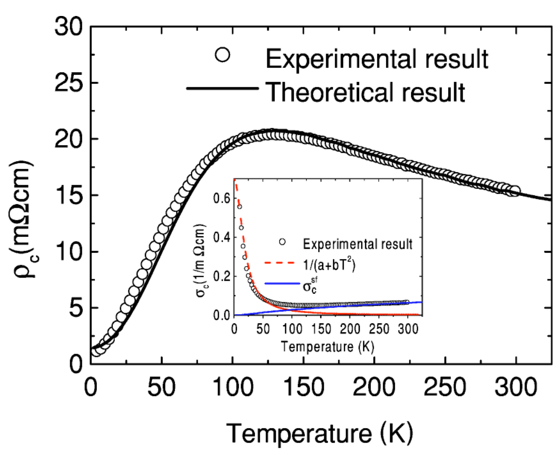


FIG. 3. Out-of-plane resistivity $\rho_c$ vs temperature $T$: open circles are the experimental data (from Ref. 2), while solid lines are the theoretical results. The inset displays the contributions of $\sigma_c^{\mathrm{SF}}$ and $\sigma_c^n = 1/(a + bT^2)$ with $a = 1.43$ m$\Omega$ cm and $b = 4.08 \times 10^{-3}$ m$\Omega$ cm/K$^2$ separately, together with the experimental results ($\sigma_c \equiv 1/\rho_c$).

tween the curves of $\rho_n(T)$ and $\rho_{\rm SF}^{\gamma}(T)$ at $T_{\rm cross}\simeq 160$ K, near which out-of-plane resistivity $\rho_c$ emerges a broad peak (see Fig. 3).

We next examine the *c*-axis resistivity anomaly. From the outcome of *ab*-plane resistivity studies, that is, there is a strong coupling between the carriers of $\gamma$ band and the incommensurate spin fluctuations, it is naturally expected that the similar coupling between the carriers of $\gamma$ band and the incommensurate spin fluctuations also dominates the *c*-axis electronic conductivity in $Sr_2RuO_4$. Following Ref. 2, we adopt the model with two (coherent and incoherent) parallel conduction channels for the *c*-axis electronic conductivity $\sigma_c$. Accordingly, $\sigma_c \equiv \sigma_c^n + \sigma_c^{\rm SF}$, where $\sigma_c^n = 1/(a+bT^2)$ corresponds to band-like contribution, while $\sigma_c^{\rm SF}$ corresponds to electronic conductivity due to the hopping assisted by incommensurate spin fluctuations, which contains the contribution of $\gamma$ band only. Simple band-transport analysis in conjunction with individual Fermi surface parameters (see Ref. 14, for example) reveal that the correlation length $l_c$ along *c*-axis are roughly 3, 36, and 30 Å for $\alpha$, $\beta$, and $\gamma$ bands, respectively. Because $l_c^{\alpha} < d = 6.3$ Å ($d$ is the interlayer distance), the coherent *c*-axis transport of $\alpha$ band is suppressed and as a result, $\sigma_c^n$ is mainly contributed by $\gamma$ and $\beta$ bands. Similar to Ref. 15, $\sigma_c^{\rm SF}$ can be calculated via

$$\sigma_{\rm c}^{\rm SF}(T) \propto \frac{J_\perp^2}{T} \sum_{\mathbf{k}\cdot\mathbf{q}} \chi''(\mathbf{k}, \varepsilon_{\mathbf{q}}^{(1)} - \varepsilon_{\mathbf{k+q}}^{(2)}) f(\varepsilon_{\mathbf{k+q}}^{(2)})[1 - f(\varepsilon_{\mathbf{k+q}}^{(2)})] \times [f(\varepsilon_{\mathbf{q}}^{(1)}) + n_B(\varepsilon_{\mathbf{q}}^{(1)} - \varepsilon_{\mathbf{k+q}}^{(2)})], \tag{5}$$

where $J_\perp$ is the effective interaction constant, $\varepsilon_{\mathbf{k}}^{(i)}$ is the band energy dispersion for layer $i$, and $\chi''(\mathbf{k},\omega)$ is the spin fluctuation spectral function given in Eq. (2) (where we shall consider only the *intralayer* spin correlation). For this type of calculation, only two neighboring layers are involved. The fit to the experimental data, taken from Ref. 2, is shown in Fig. 3. The best fit is obtained for $a = 1.43$ m$\Omega$ cm and $b = 4.08 \times 10^{-3}$ m$\Omega$ cm/K$^2$. Fairly good agreement between the experimental result and the theoretical prediction indicates that the ISF does indeed influence the *c*-axis electronic conductivity and leads to anomalous behavior of $\rho_c$.

In the literature, there are other approaches which theoretically investigate the normal-state in-plane $\rho_{ab}$ and out-of-plane $\rho_c$ resistivities of $Sr_2RuO_4$.[3–5] Two major mechanisms are usually assumed. One common mechanism for both $\rho_{ab}$ and $\rho_c$ is the bandlike contribution which originates mainly from the scattering of the electrons by impurities and by other electrons, for which there has been a consensus on its importance. As for the second dominant mechanism, the views differ for $\rho_{ab}$ and $\rho_c$. As an example, Ref. 5 considers $\rho_{ab}$ to be attributed to ferromagnetic spin fluctuations, while for $\rho_c$, they[5] suggest that it might be due to the thermally assisted hopping. In our case, we suggest that the novel behavior of $\rho_{ab}$ is due to the coupling between the carriers of $\gamma$ band and the ISF, which is *also* responsible for the novel behavior of $\rho_c$.

It is worthwhile to remark our fitting process for $\rho_{ab}$ and $\rho_c$. For $\rho_{ab}$, because of the experimental fact of no residual resistivity at $T=0$ (and thus $a=0$), the number of fitting parameter is 2 ($b$ and $J$). Relative value of $b$ and $J$ represents the relative contribution attributed to Fermi liquid and ISF. For $\rho_c$, on the other hand, the number of fitting variables is 3 ($a$, $b$, and $J_\perp$). The parameters $a$ and $b$ represent the relative contribution due to impurity and electron-electron scattering, while $J_\perp$ represents the contribution of the hopping assisted by ISF. Secondly, our main focus is to study the effect of temperature on the resistivities, so we have omitted the constants ($e$, $k_B$, etc.) in Eqs. (1) and (5), leaving the fitting parameters $J$ and $J_\perp$ to arbitrary units. To determine the physical values of $J$ and $J_\perp$, one at least needs to know the carrier concentration of $\gamma$ band (through the study of a different observable quantity), which is not available at this stage. Finally, it is reminded that we consider only the intralayer spin correlation (i.e., the interlayer spin correlation is neglected) and have used the same spin-fluctuation spectral function [Eq. (2)] for both $\rho_{ab}$ and $\rho_c$ calculations.

To test our scenario, we suggest using the pressure experiment. Recent resistivity measurements under pressure done by Yoshida *et al.*[5] and Shirakawa *et al.*[16] for $Sr_2RuO_4$ reported that at high temperatures, $\rho_{ab}$ decreases, while $\rho_c$ increases, as pressure increases. In addition, Yoshida *et al.*[5] also reported that the temperature $T_M$, where $\rho_c$ develops a peak, increases as pressure increases. This sets a strong constraint on the theoretical model. How the pressure affects the values of $\rho_{\rm SF}$, $\sigma_c^{\rm SF}$, the spectral function $\chi''$, and many others remains to be investigated. In the following, we instead make some heuristic calculations. For $\rho_{ab}$, we decrease both the weights of $T^2$ term and $\rho_{\rm SF}(T)$ by 30% and then add a constant ($a = 4$ $\mu\Omega$ cm) to it. The suppression of $\rho_{\rm SF}(T)$ corresponds to the decrease of spin fluctuation spectral weight at $\mathbf{Q}_i$ under pressure, which we believe to be of the most importance. While the decrease of $T^2$ term occurs be-

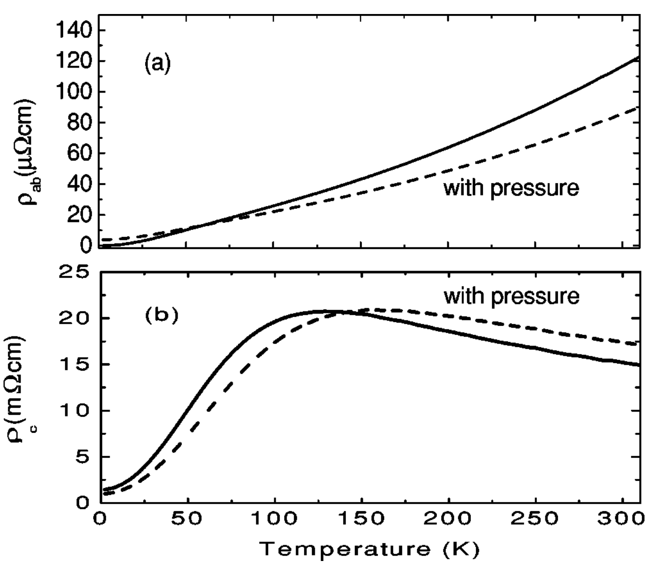


FIG. 4. Numerical results: (a) $\rho_{ab}(T)$ with different weights of $\rho_{\rm SF}(T)$ and $\rho_n(T)$; (b) $\rho_c(T)$ with different weights of $\sigma_c^{\rm SF}(T)$ and $\sigma_c^n(T)$. In both frames, dash lines are the corresponding curves with applied pressure. See text for more detailed description.

cause pressure suppresses the electron-electron interaction (see experiment of Ref. 17, for example). Due to pressure, there emerges a constant term associated with impurity scattering.[17] For $\rho_c$, in contrast, we increase the weight of $\sigma_c^n$ by 45% (which mimics the increase of electronic conductivity of the bandlike term) and decrease the weight of $\sigma_c^{\mathrm{SF}}$ by 15% (which mimics the decrease of the electronic conductivity associated with the hopping assisted by ISF).

Numerical results for $\rho_{ab}$ and $\rho_c$ versus $T$ with the new weighting (dashed lines) are shown in Figs. 4(a) and 4(b), where original curves (already given in Figs. 2 and 3) are included for comparison (solid lines). As seen in Fig. 4(a), at high temperatures the resistivity under pressure is *lower* than the no pressure one. In other words, if pressure can alter the weights of $T^2$ and $\rho_{\mathrm{SF}}(T)$ in $\rho_{ab}$ as we assumed, $\rho_{ab}$ then decreases as the pressure increases. In addition, we predict a cross point between the curves with and without pressure, which is resulting from the impurity scattering induced by the pressure. While in Fig. 4(b), we see the pressure alter the weights of $\sigma_c^n$ and $\sigma_c^{\mathrm{SF}}$, and as a result, the peak temperature $T_M$ increases as the pressure increases. Moreover, at low temperatures, $\rho_c$ decreases as the pressure increases; at high temperatures, in contrast, $\rho_c$ increases as the pressure increases.

If we accept the results of the above model calculation associated with pressure, we can understand not only how pressure makes $\rho_{ab}$ decrease at high temperatures, and $\rho_c$ increase at high temperatures and decrease at low temperatures, but also the peak temperature $T_M$ in $\rho_c$ increases as pressure increases . The cross point in Fig. 4(a) for $\rho_{ab}$ remains to be seen. Apparently, our model gives a very favorable account when comparing with experiments. It is thus highly demanded that the INS experiment under different pressures be performed to check whether pressure suppresses the strength of the incommensurate spin-fluctuation spectral function at $\mathbf{Q}_i$ for $Sr_2RuO_4$. Of course, we also hope that more data on electrical resistivity will be done in order to compare with our model.

In summary, in this report we have studied the normal-state transport properties of $Sr_2RuO_4$ for both in-plane and out-of-plane resistivity ($\rho_{ab}$ and $\rho_c$). We have shown that, assuming there is a strong coupling between the carriers of $\gamma$ band and the incommensurate spin fluctuations (in addition to the normal scattering of electrons by impurities and by other electrons), the temperature variations of $\rho_{ab}$ and $\rho_c$ of $Sr_2RuO_4$ are governed by the incommensurate spin fluctuation, whose effect is observed to cover a wide temperature range. Based on these results, we argue that there is a strong coupling between the carriers of $\gamma$ band and the incommensurate spin fluctuations in $Sr_2RuO_4$. It is due to this coupling that leads to the anomalous behaviors of $\rho_{ab}$ and $\rho_c$ in $Sr_2RuO_4$.

This work was supported by the NSC of Taiwan under Grant Nos. 91-2112-M-003-019 and 91-2112-M-003-020, and by the National Natural Science Foundation of P.R. China under Grant No. 19974001 and the Education Commission of Anhui.

[1] Y. Maeno, H. Hashimoto, K. Yoshida, S. Nishizaki, T. Fujita, J.G. Bednorz, and F. Lichtenberg, Nature (London) **372**, 532 (1994).
[2] N.E. Hussey, A.P. Mackenzie, J.R. Cooper, Y. Maeno, S. Nishizaki, and T. Fujita, Phys. Rev. B **57**, 5505 (1998).
[3] C. Noce, G. Busiello, and M. Cuoco, Europhys. Lett. **51**, 195 (2000).
[4] C. Noce and M. Cuoco, Phys. Rev. B **62**, 9884 (2000).
[5] K. Yoshida, F. Nakamura, T. Goko, T. Fujita, Y. Maeno, Y. Mori, and S. Nishizaki, Phys. Rev. B **58**, 15 062 (1998).
[6] Y. Sidis, M. Braden, P. Bourges, B. Hennion, S. Nishizaki, Y. Maeno, and Y. Mori, Phys. Rev. Lett. **83**, 3320 (1999).
[7] M. Braden, Y. Sidis, P. Bourges, P. Pfeuty, J. Kulda, Z. Mao, and Y. Maeno, Phys. Rev. B **66**, 064522 (2002).
[8] I.I. Mazin and D.J. Singh, Phys. Rev. Lett. **82**, 4324 (1999).
[9] N. W. Ashcroft and N. D. Mermin, *Solid State Physics* (Saunders College Publishing, Philadelphia, 1976), p. 348.
[10] W. Gotze and P. Wolfle, Phys. Rev. B **6**, 1226 (1972).
[11] T. Moriya and Y. Takahashi, J. Phys. Soc. Jpn. **60**, 776 (1991).
[12] B. Arfi, Phys. Rev. B **45**, 2352 (1992).
[13] D.K. Morr, P.F. Trautman, and M.J. Graf, Phys. Rev. Lett. **86**, 5978 (2001).
[14] A.P. Mackenzie, S.R. Julian, A.J. Diver, G.J. McMullan, M.P. Ray, G.G. Lonzarich, Y. Maeno, S. Nishizaki, and T. Fujita, Phys. Rev. Lett. **76**, 3786 (1996).
[15] Ping Lou, Phys. Rev. B **65**, 214511 (2002).
[16] N. Shirakawa, K. Murata, S. Nishizaki, Y. Maeno, and T. Fujita, Phys. Rev. B **56**, 7890 (1997).
[17] D. Forsythe, S.R. Julian, C. Bergemann, E. Pugh, M.J. Steiner, P.L. Alireza, G.J. McMullan, F. Nakamura, R.K.W. Haselwimmer, I.R. Walker, S.S. Saxena, G.G. Lonzarich, A.P. Mackenzie, Z.Q. Mao, and Y. Maeno, Phys. Rev. Lett. **89**, 166402 (2002).